

Spin-dependent WIMP scattering off nuclei

J. Menéndez,^{1,2} D. Gazit,³ and A. Schwenk^{2,1}

¹*Institut für Kernphysik, Technische Universität Darmstadt, 64289 Darmstadt, Germany*

²*ExtreMe Matter Institute EMMI, GSI Helmholtzzentrum für Schwerionenforschung GmbH, 64291 Darmstadt, Germany*

³*Racah Institute of Physics and The Hebrew University Center for Nanoscience and Nanotechnology, The Hebrew University, 91904 Jerusalem, Israel*

Chiral effective field theory (EFT) provides a systematic expansion for the coupling of WIMPs to nucleons at the momentum transfers relevant to direct cold dark matter detection. We derive the currents for spin-dependent WIMP scattering off nuclei at the one-body level and include the leading long-range two-body currents, which are predicted in chiral EFT. As an application, we calculate the structure factor for spin-dependent WIMP scattering off ^{129,131}Xe nuclei, using nuclear interactions that have been developed to study nuclear structure and double-beta decays in this region. We provide theoretical error bands due to the nuclear uncertainties of WIMP currents in nuclei.

PACS numbers: 95.35.+d, 12.39.Fe, 21.60.Cs

I. INTRODUCTION

Cosmological and astrophysical observations have established that more than 20% of the energy density of our universe is dark matter, a rarely interacting nonbaryonic form of matter, whose specific composition remains unknown [1]. Promising candidates are weakly interacting massive particles (WIMPs), such as neutralinos, the lightest supersymmetric particles predicted by extensions of the standard model. This has spurred direct detection of cold dark matter via elastic scattering off nuclei, requiring detailed knowledge of the response to WIMP induced currents in nuclei. This presents a challenging problem, because even if the coupling of neutralinos (or other particles) to quarks is known, it needs to be evaluated at the nucleus level in the nonperturbative regime of quantum chromodynamics [2].

Chiral effective field theory (EFT) provides a systematic expansion for nuclear forces and the coupling to external probes for momenta of order of the pion mass, $p \sim m_\pi \sim 100$ MeV, which are typical momentum transfers in direct dark matter detection. In this paper, we focus on spin-dependent neutralino scattering off nuclei, which is used to constrain WIMP properties [3] and is particularly sensitive to nuclear structure. We derive the currents for spin-dependent WIMP scattering at the one-body level and include the leading long-range two-nucleon currents, which are predicted in chiral EFT. Similar weak neutral currents are key for providing accurate predictions of neutrino breakup of the deuteron for SNO [4], while the corresponding weak charged currents have been found relevant in Gamow-Teller and double-beta decays of medium-mass nuclei [5].

We apply the developed chiral EFT currents to calculate the structure factor for spin-dependent WIMP scattering off ^{129,131}Xe, as xenon isotopes provide the tightest limits on WIMP couplings [6]. To describe these nuclei, we employ the largest many-body spaces accessible with nuclear interactions previously used to study nuclear structure and double-beta decays in this region [7].

II. SPIN-DEPENDENT INTERACTIONS

We focus on spin-dependent WIMP scattering, for which the low-momentum-transfer Lagrangian density \mathcal{L} is taken to be a spatial axial-vector-axial-vector coupling [8, 9],

$$\mathcal{L} = -\frac{G_F}{\sqrt{2}} \bar{\chi} \gamma_5 \chi \cdot \sum_q A_q \bar{\psi}_q \gamma_5 \psi_q, \quad (1)$$

where G_F is the Fermi coupling constant, χ the neutralino field, ψ_q the fields of $q = u, d, s$ quarks, and A_q are neutralino-quark coupling constants. At the one-nucleon level, the quark currents are replaced by their expectation value in a single nucleon. This leads to one-body (1b) axial-vector currents $\mathbf{J}_{i,1b}$. Summing over all A nucleons in a nucleus, one has [8]

$$\begin{aligned} \sum_q A_q \bar{\psi}_q \gamma_5 \psi_q &\longrightarrow \sum_{i=1}^A \mathbf{J}_{i,1b} = \sum_{i=1}^A (\mathbf{J}_{i,1b}^0 + \mathbf{J}_{i,1b}^3) \\ &= \sum_{i=1}^A \frac{1}{2} \left[a_0 \boldsymbol{\sigma}_i + a_1 \tau_i^3 \left(\boldsymbol{\sigma}_i - \frac{g_F(p^2)}{2mg_A} (\mathbf{p} \cdot \boldsymbol{\sigma}_i) \mathbf{p} \right) \right], \quad (2) \end{aligned}$$

where $\mathbf{p} = \mathbf{p}_i - \mathbf{p}'_i$ denotes the momentum transfer from nucleons (with mass m) to neutralinos. The isoscalar part $\mathbf{J}_{i,1b}^0$ with coupling $a_0 = (A_u + A_d)(\Delta u + \Delta d) + 2A_s \Delta s$ receives contributions from the isoscalar combination of the u and d quarks to the spin of the nucleon, as well as from the s quark. Here Δq denotes the matrix element of $\bar{\psi}_q \gamma_5 \psi_q$ in the nucleon up to the spin $\boldsymbol{\sigma}/2$ [8]. The isovector coupling can be written as $a_1 = (A_u - A_d)(\Delta u - \Delta d) = (A_u - A_d)g_A$, with the axial coupling constant g_A . Therefore the isovector part $\mathbf{J}_{i,1b}^3$ of the axial-vector WIMP coupling to the nucleon is up to a factor g_A identical to the axial-vector part of the weak neutral current.

III. CHIRAL EFT AND WIMP CURRENTS

The weak neutral current was derived within chiral EFT for calculations of low-energy electroweak reactions. At order Q^0 and Q^2 , there are only one-body currents, which for the isovector part of the axial-vector WIMP current lead to

$$\mathbf{J}_{i,1b}^3 = \frac{1}{2} a_1 \tau_i^3 \left(\frac{g_A(p^2)}{g_A} \boldsymbol{\sigma}_i - \frac{g_P(p^2)}{2m g_A} (\mathbf{p} \cdot \boldsymbol{\sigma}_i) \mathbf{p} \right). \quad (3)$$

In chiral EFT, the p dependence of the axial and pseudo-scalar couplings $g_A(p^2)$ and $g_P(p^2)$ is due to loop corrections and pion propagators, to order Q^2 [10]:

$$\frac{g_A(p^2)}{g_A} = 1 - 2 \frac{p^2}{\Lambda_A^2} \quad \text{and} \quad g_P(p^2) = \frac{2g_{\pi pn} F_\pi}{m_\pi^2 + p^2} - 4 \frac{m g_A}{\Lambda_A^2}, \quad (4)$$

with $\Lambda_A = 1040$ MeV, pion mass $m_\pi = 138.04$ MeV, pion decay constant $F_\pi = 92.4$ MeV, and $g_{\pi pn} = 13.05$. In previous calculations of WIMP scattering off nuclei, the smaller $1/\Lambda_A^2$ terms are generally neglected and the Goldberger-Treiman relation is implicitly used to write $\frac{g_P(p^2)}{2m g_A} \approx \frac{1}{m_\pi^2 + p^2}$ (compare with Ref. [8]).

Neglecting the strange quark contribution, the neutral axial-vector currents are isovector in the Standard Model. Therefore, knowledge of the isoscalar currents in the nucleon is based on models. These suggest that the Q^2 one-body currents have a form-factor mass-scale $\sim \Lambda_A$ [11]. Because the isovector $1/\Lambda_A^2$ terms contribute at the few percent level to spin-dependent WIMP scattering, we do not attempt to model these and neglect higher-order isoscalar current contributions.

IV. TWO-BODY CURRENTS

At order Q^3 , two-body (2b) currents enter in chiral EFT [12]. For spin-independent WIMP scattering, the potential impact of meson-exchange currents has been pointed out in Ref. [13]. In chiral EFT, the long-range parts of 2b currents are predicted. Because of their pion-exchange nature, they only have an isovector part, $\mathbf{J}_{2b} = \sum_{i < j}^A \mathbf{J}_{ij}^3$. For the axial-vector weak neutral current, this leads to

$$\mathbf{J}_{12}^3 = -\frac{g_A}{2F_\pi^2} \frac{1}{m_\pi^2 + k^2} \left[\left(c_4 + \frac{1}{4m} \right) \mathbf{k} \times (\boldsymbol{\sigma}_\times \times \mathbf{k}) \tau_\times^3 + 2c_3 \mathbf{k} \cdot (\boldsymbol{\sigma}_1 \tau_1^3 + \boldsymbol{\sigma}_2 \tau_2^3) \mathbf{k} - \frac{i}{2m} \mathbf{k} \cdot (\boldsymbol{\sigma}_1 - \boldsymbol{\sigma}_2) \mathbf{q} \tau_\times^3 \right], \quad (5)$$

where $\tau_\times^3 = (\tau_1 \times \tau_2)^3$ and the same for $\boldsymbol{\sigma}_\times$, $\mathbf{k} = \frac{1}{2}(\mathbf{p}'_2 - \mathbf{p}_2 - \mathbf{p}'_1 + \mathbf{p}_1)$ and $\mathbf{q} = \frac{1}{4}(\mathbf{p}_1 + \mathbf{p}'_1 - \mathbf{p}_2 - \mathbf{p}'_2)$. The low-energy couplings c_3, c_4 relate different processes and are determined in the pion-nucleon or nucleon-nucleon systems [14].

Following Ref. [5], we include the normal-ordered 1b parts of chiral 2b currents. This is expected to be a very

good approximation in medium-mass and heavy nuclei, because of phase-space arguments [15]. We sum the second nucleon over occupied states in a spin and isospin symmetric reference state or core: $\mathbf{J}_{i,2b}^{\text{eff}} = \sum_j (1 - P_{ij}) \mathbf{J}_{ij}^3$, where P_{ij} is the exchange operator. Taking a Fermi gas approximation for the core we obtain the normal-ordered 1b current. This contains two terms. First, it leads to an in-medium renormalization of the axial coupling [5]:

$$\mathbf{J}_{i,2b}^{\text{eff}} = -g_A \boldsymbol{\sigma}_i \frac{\tau_i^3}{2} \frac{\rho}{F_\pi^2} I(\rho, P = 0) \left(\frac{1}{3} (2c_4 - c_3) + \frac{1}{6m} \right), \quad (6)$$

with total momentum $\mathbf{P} = \mathbf{p}_i + \mathbf{p}'_i$. The P dependence is very weak ($< 15\%$) from $P = 0$ to the Fermi-gas mean-value $P^2 = 6k_F^2/5$, and we therefore take $P = 0$ in the following. Here, $\rho = 2k_F^3/(3\pi^2)$ is the density of the reference state, k_F the corresponding Fermi momentum, and $I(\rho, P)$ is due to the summation in the exchange term,

$$I(\rho, P = 0) = 1 - \frac{3m_\pi^2}{k_F^2} + \frac{3m_\pi^3}{2k_F^3} \text{arccot} \left[\frac{m_\pi^2 - k_F^2}{2m_\pi k_F} \right]. \quad (7)$$

Such a renormalization is also expected considering chiral 3N forces as density-dependent two-body interactions [16]. We take a typical range for the densities in nuclei $\rho = 0.10 \dots 0.12 \text{ fm}^{-3}$. This leads to $I(\rho, P = 0) = 0.58 \dots 0.60$. The resulting 2b contribution to the axial-vector WIMP current can be included as a density-dependent renormalization $a_1(1 + \delta a_1)$, with

$$\delta a_1 \equiv -\frac{\rho}{F_\pi^2} I(\rho, P = 0) \left(\frac{1}{3} (2c_4 - c_3) + \frac{1}{6m} \right). \quad (8)$$

Normal ordering leads to a second contribution which renormalizes the pseudo-scalar coupling. At $P = 0$, this takes the form for the weak neutral current

$$\mathbf{J}_{i,2b}^{\text{eff}, P} = -g_A \tau_i^3 \frac{\rho}{F_\pi^2} c_3 \frac{(\mathbf{p} \cdot \boldsymbol{\sigma}_i) \mathbf{p}}{4m_\pi^2 + p^2}. \quad (9)$$

For neutrinoless double-beta decay, we approximated $(\mathbf{p} \cdot \boldsymbol{\sigma}_i) \mathbf{p} \rightarrow p^2/3 \boldsymbol{\sigma}_i$, which neglects the small tensor part between 0^+ ground states [5]. For the axial-vector WIMP current, we fully include the contribution of Eq. (9) via a density- and momentum-dependent modification of the pseudo-scalar part. To this end, we define

$$\delta a_1^P(p^2) \equiv -2c_3 \frac{\rho}{F_\pi^2} \frac{p^2}{4m_\pi^2 + p^2}. \quad (10)$$

In addition to the long-range pion-exchange currents, there are short-range 2b currents both for the isoscalar and isovector parts, which are included as contact terms in chiral EFT. For Gamow-Teller transitions, which are an isospin rotation of the axial-vector WIMP currents, the contributions from long-range 2b currents were found to dominate over the short-range parts in medium-mass to heavy nuclei (for typical short-range couplings c_D), because c_3, c_4 are large in chiral EFT without explicit Deltas [5]. Therefore, we neglect the short-range 2b current contributions here, consistently with neglecting higher-order 1b isoscalar currents, as discussed above.

V. WIMP-NUCLEUS SCATTERING

The differential cross-section for spin-dependent WIMP elastic scattering on a nucleus in the ground state with total angular momentum J is given by [8]

$$\frac{d\sigma}{dp^2} = \frac{8G_F^2}{(2J+1)v^2} S_A(p), \quad (11)$$

where v is the WIMP velocity and $S_A(p)$ is the axial-vector structure factor, which can be decomposed as

$$S_A(p) = \sum_{L \text{ odd}} \left(|\langle J || \mathcal{T}_L^{\text{el}5}(p) || J \rangle|^2 + |\langle J || \mathcal{L}_L^5(p) || J \rangle|^2 \right). \quad (12)$$

The sum is over multipoles L with reduced matrix elements of the transverse electric $\mathcal{T}_L^{\text{el}5}$ and longitudinal \mathcal{L}_L^5 projections of the axial-vector currents. These can be expanded in vector spherical harmonics [8, 17], leading to

$$\mathcal{T}_L^{\text{el}5}(p) = \frac{1}{\sqrt{2L+1}} \sum_{i=1}^A \frac{1}{2} \left[a_0 + a_1 \tau_i^3 \left(1 - 2 \frac{p^2}{\Lambda_A^2} + \delta a_1 \right) \right] \times \left[-\sqrt{L} M_{L,L+1}(p\mathbf{r}_i) + \sqrt{L+1} M_{L,L-1}(p\mathbf{r}_i) \right], \quad (13)$$

$$\mathcal{L}_L^5(p) = \frac{1}{\sqrt{2L+1}} \sum_{i=1}^A \times \frac{1}{2} \left[a_0 + a_1 \tau_i^3 \left(1 + \delta a_1 - \frac{2g_{\pi pn} F_\pi p^2}{2mg_A(m_\pi^2 + p^2)} + \delta a_1^P(p^2) \right) \right] \times \left[\sqrt{L+1} M_{L,L+1}(p\mathbf{r}_i) + \sqrt{L} M_{L,L-1}(p\mathbf{r}_i) \right]. \quad (14)$$

Expressions for $M_{L,L'}(p\mathbf{r}_i) = j_{L'}(pr_i)[Y_{L'}(\hat{\mathbf{r}}_i) \boldsymbol{\sigma}_i]^L$ (with L' and $\boldsymbol{\sigma}$ coupled to L) are given in Ref. [17]. The pseudo-scalar currents do not contribute to the transverse electric multipoles, and for the longitudinal part, one can replace $(\mathbf{p} \cdot \boldsymbol{\sigma}_i) \mathbf{p} \rightarrow p^2 \boldsymbol{\sigma}_i$. As a result, the p^2/Λ_A^2 terms in the longitudinal response cancel [see Eq. (4)] and only contribute to the transverse electric multipoles.

VI. NUCLEAR STRUCTURE AND RESULTS

We carry out state-of-the-art large-scale shell-model calculations for the structure of ^{129}Xe and ^{131}Xe . The valence space for both protons and neutrons comprises the $0g_{7/2}$, $1d_{5/2}$, $1d_{3/2}$, $2s_{1/2}$, and $0h_{11/2}$ orbitals on top of a ^{100}Sn core. In the case of ^{129}Xe , the number of particles in the $1d_{3/2}$, $2s_{1/2}$, and $0h_{11/2}$ orbitals was limited to 3, in order to make the calculations feasible (the matrix dimension for this space is 3.5×10^8). We have used the so-called gcn5082 interaction [7], which is based on a G-matrix with empirical adjustments, mainly in the monopole part, to describe nuclei within this region. The same interaction and valence space have been used to study structure and double-beta decays. Calculations have been performed with the shell-model code ANTOINE [18].

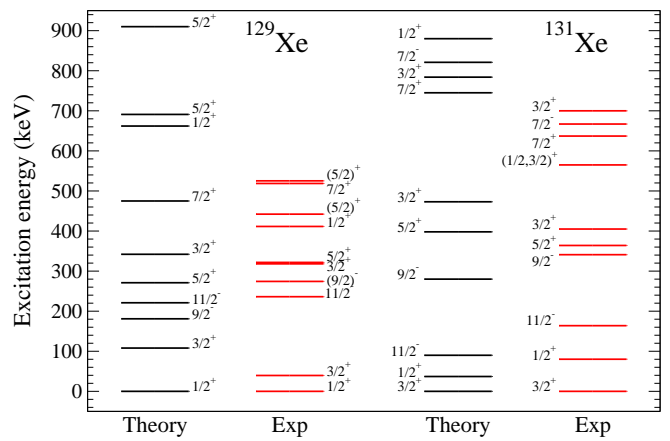


FIG. 1. (Color online) Comparison of calculated spectra of ^{129}Xe and ^{131}Xe with experiment. The interaction and valence space are the same as in structure and double-beta decay studies in this region [7]. The ^{131}Xe diagonalization is in the full space, while the ^{129}Xe case was restricted (see text).

A fully consistent treatment of the one- and two-body currents would require to renormalize them to the valence space of the many-body calculation, which can lead to additional contributions to the currents. This will be pursued in future work. In this first application, we focus on the effects of the bare chiral currents.

Figure 1 shows the resulting spectra for ^{129}Xe and ^{131}Xe , measured from the ground-state energy. In both cases, the experimental ground state and the overall ordering of the excited states are remarkably well described, which represents a clear improvement with respect to previous work [19]. This reflects the quality of the interaction and valence space used. The resulting magnetic moments, with standard g factors for this region [20], are $\mu = -0.72\mu_N$ and $0.86\mu_N$ for ^{129}Xe and ^{131}Xe , respectively, which agree within $\sim 20\%$ with experiment. However, we emphasize that the magnetic moments probe different physics, as the axial-vector WIMP couplings at $p = 0$ are an isospin rotation of the Gamow-Teller operator, not a coupling to magnetic moments. In fact, one could fine-tune the effective g factors to improve the agreement with magnetic moments (which is sometimes pursued [19]), but this leaves the predicted axial-vector structure factor unchanged.

In the limit of low momentum-transfer, $p = 0$, the axial-vector structure factor reduces to the expectation values of the total proton and neutron spin operators, $\mathbf{S}_p = \sum_{i=1}^Z \boldsymbol{\sigma}_i/2$ and $\mathbf{S}_n = \sum_{i=1}^N \boldsymbol{\sigma}_i/2$,

$$S_A(0) = \frac{1}{4\pi} \left| (a_0 + a'_1) \langle J || \mathbf{S}_p || J \rangle + (a_0 - a'_1) \langle J || \mathbf{S}_n || J \rangle \right|^2, \quad (15)$$

where $a'_1 = a_1(1 + \delta a_1)$ includes the effects from chiral 2b currents. For the expectation values $\langle \mathbf{S}_{n,p} \rangle = \langle JM =$

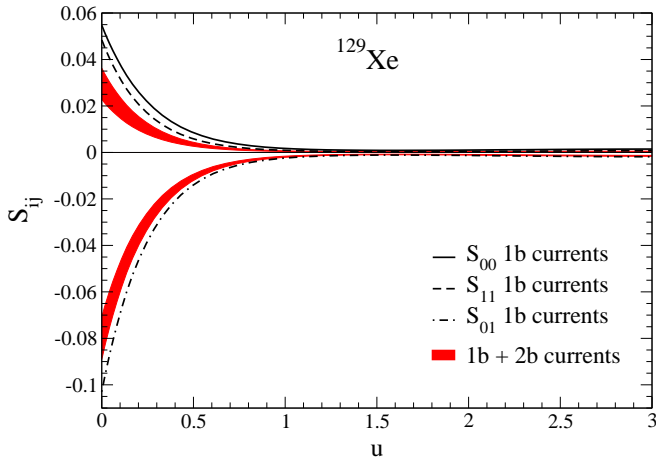


FIG. 2. (Color online) Structure factors S_{00} , S_{11} and S_{01} for ^{129}Xe as a function of $u = p^2 b^2 / 2$, with harmonic-oscillator length $b = 2.2853$ fm. Results are shown at the one-body (1b) current level, and for the isovector and isoscalar-isovector factors S_{11} and S_{01} also including two-body (2b) currents. The estimated theoretical uncertainty is given by the red band.

$J|\mathbf{S}_{n,p}^3|JM = J\rangle$, we obtain

	^{129}Xe	^{131}Xe
$\langle \mathbf{S}_n \rangle$	0.329	-0.272
$\langle \mathbf{S}_p \rangle$	0.010	-0.009

As expected for odd-mass nuclei with even number of protons, $\langle \mathbf{S}_n \rangle \gg \langle \mathbf{S}_p \rangle$. The predicted spin expectation values are qualitatively similar to those of Ressel and Dean [21], who considered two different (Bonn A/Nijmegen II) interactions, although their $\langle \mathbf{S}_p \rangle = 0.013/0.028$ for ^{129}Xe is larger and their $\langle \mathbf{S}_n \rangle$ values for ^{131}Xe are 20% smaller. The results of Toivanen *et al.* [19] differ substantially, as expected based on their poor reproduction of the spectra. They give 15%/55% smaller $\langle \mathbf{S}_n \rangle$ values for $^{129}\text{Xe}/^{131}\text{Xe}$ and both $\langle \mathbf{S}_p \rangle$ values an order of magnitude smaller (for ^{129}Xe also of opposite sign). We attribute these differences to the sizeable truncations of the valence spaces in Refs. [19, 21] and also because the nuclear interactions are not as well tested compared to this work.

At finite p , one introduces isoscalar/isovector (0/1) structure factors $S_{00}(p)$, $S_{01}(p)$ and $S_{11}(p)$ through

$$S_A(p) = a_0^2 S_{00}(p) + a_0 a_1 S_{01}(p) + a_1^2 S_{11}(p). \quad (17)$$

Figures 2 and 3 show the predicted structure factors for ^{129}Xe and ^{131}Xe as a function of $u = p^2 b^2 / 2$, with harmonic-oscillator length $b = (\hbar/m\omega)^{1/2}$ and $\hbar\omega = (45A^{-1/3} - 25A^{-2/3})$ MeV. Fits to S_{00} , S_{11} and S_{01} are provided in Table I.

At the 1b level at order Q^2 , the results shown correspond to the same current operator as in Refs. [19, 21], but based on chiral EFT couplings and with the $1/\Lambda_A^2$ term in g_A and g_P included. Since $\langle \mathbf{S}_n \rangle$ sets the scale for the $p = 0$ response, one has $S_{00} \approx S_{11} \approx -1/2 S_{01}$.

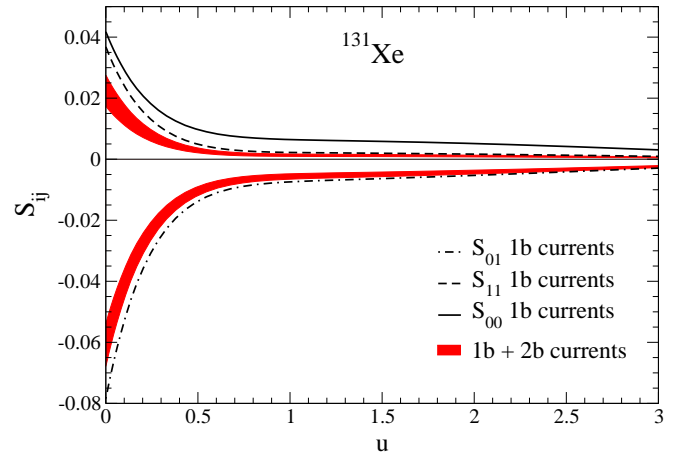


FIG. 3. (Color online) Structure factors S_{00} , S_{11} and S_{01} for ^{131}Xe as a function of $u = p^2 b^2 / 2$, with harmonic-oscillator length $b = 2.2905$ fm. The labels are as in Fig. 2.

Thus, our response is about 35% larger for ^{131}Xe compared to Ressel and Dean [21], and about 30%/4 times larger for $^{129}\text{Xe}/^{131}\text{Xe}$ than Toivanen *et al.* [19]. For $p \gtrsim m_\pi$, $u \gtrsim 1.3$, the structure factors nearly vanish for ^{129}Xe , similar to Refs. [19, 21], as expected for a $1/2^+$ ground state, where only $L = 1$ multipoles contribute. For ^{131}Xe , the predicted structure factors remain nonvanishing but small, similar to Ressel and Dean [21]. Both differ significantly from Toivanen *et al.* [19] suggesting very different higher $L = 3$ multipole contributions.

When chiral 2b currents are included at order Q^3 , we provide theoretical error bands in Figs. 2 and 3 due to the nuclear uncertainties in WIMP currents in nuclei. This takes into account the uncertainties in the low-energy couplings c_3, c_4 (with the conservative range used in Ref. [5]) as well as the range in nuclear densities $\rho = 0.10 \dots 0.12$ fm $^{-3}$. Chiral 2b currents provide important contributions to the structure factors, especially for $p \lesssim 100$ MeV, $u \lesssim 0.7$, where their effects are to significantly reduce, by about 25–55%, the isovector S_{11} factor, similar to the Gamow-Teller quenching [5] and by about half of that the isoscalar-isovector S_{01} factor, compared to the results at the 1b level at order Q^2 .

For $p \gtrsim m_\pi$, the effects of 2b currents are expected to be smaller due to the momentum-dependent modification of the pseudo-scalar part of the current, $\delta a_1^P(p^2)$, which has opposite sign compared to the leading 1b contribution (see Eq. (10) with $c_3 < 0$ [5]). This term, however, only affects the longitudinal multipoles, leading to a nucleus-dependent reduction. For ^{129}Xe , most of the response comes from the transverse electric multipoles, so that the relative contribution from chiral 2b currents is approximately p independent. For ^{131}Xe , at $p \sim 250$ MeV the relative effect of chiral 2b currents is $\sim 10 - 15\%$ smaller than at $p \sim 100$ MeV, in agreement with the momentum-transfer dependence of chiral 2b currents found in Gamow-Teller transitions [5].

As discussed, the 2b current contributions to the isoscalar S_{00} factor are small and are not considered here. The chiral 2b current contributions should be included in all calculations of spin-dependent elastic and inelastic WIMP scattering off nuclei. The effects of 2b currents are expected to be smaller for the vector structure factor and thus for the spin-independent elastic WIMP response.

VII. SUMMARY

This presents the first calculation of spin-dependent WIMP currents in nuclei based on chiral EFT, including the leading long-range 2b currents. They predict a 25 – 55% reduction of the isovector part of the one-body axial-vector WIMP currents, where the range provides an estimate of the theoretical uncertainties of WIMP currents in nuclei. This should be included in limits on

the WIMP couplings, where the spin-dependent analysis provides complementary constraints [3]. As an application, we have calculated the structure factors for spin-dependent WIMP scattering off $^{129,131}\text{Xe}$ nuclei, using the largest valence spaces accessible with nuclear interactions that have been tested in nuclear structure and double-beta decay studies in this region. Future work includes developing consistent interactions based on chiral EFT, where the present frontier is in the calcium region [22], and investigating other nuclei and responses.

ACKNOWLEDGMENTS

We thank L. Baudis, T. Marrodan and U.-G. Meißner for helpful discussions. This work was supported in part by the DFG through grant SFB 634, the Helmholtz Alliance HA216/EMML, and a BMBF ARCHES Award.

-
- [1] R. J. Gaitskell, *Annu. Rev. Nucl. Part. Sci.* **54**, 315 (2004); J. L. Feng, *Annu. Rev. Astron. Astrophys.* **48**, 495 (2010).
 - [2] A. L. Fitzpatrick, W. Haxton, E. Katz, N. Lubbers and Y. Xu, arXiv:1203.3542; V. Cirigliano, M. L. Graesser and G. Ovanessian, arXiv:1205.2695.
 - [3] H. S. Lee *et al.* (KIMS Collaboration), *Phys. Rev. Lett.* **99**, 091301 (2007); J. Angle *et al.* (XENON10 Collaboration), *Phys. Rev. Lett.* **101**, 091301 (2008); V. N. Lebedenko *et al.* (ZEPLIN-III Collaboration), *Phys. Rev. Lett.* **103**, 151302 (2009); E. Behnke *et al.* (COUPP Collaboration), *Phys. Rev. Lett.* **106**, 021303 (2011); S. Archambault *et al.* (PICASSO Collaboration), *Phys. Lett. B* **711**, 153 (2012); M. Felizardo *et al.* (SIMPLE Collaboration), *Phys. Rev. Lett.* **108**, 201302 (2012).
 - [4] M. Butler, J.-W. Chen and X. Kong, *Phys. Rev. C* **63**, 035501 (2001); S. Nakamura, T. Sato, V. P. Gudkov and K. Kubodera, *Phys. Rev. C* **63**, 034617 (2001).
 - [5] J. Menéndez, D. Gazit and A. Schwenk, *Phys. Rev. Lett.* **107**, 062501 (2011).
 - [6] E. Aprile *et al.* (XENON100 Collaboration), *Phys. Rev. Lett.* **107**, 131302 (2011) and arXiv:1207.5988.
 - [7] E. Caurier, J. Menéndez, F. Nowacki and A. Poves, *Phys. Rev. Lett.* **100**, 052503 (2008); J. Menéndez, A. Poves, E. Caurier and F. Nowacki, *Nucl. Phys. A* **818**, 139 (2009).
 - [8] J. Engel, S. Pittel and P. Vogel, *Int. J. Mod. Phys. E* **1**, 1 (1992).
 - [9] G. Jungman, M. Kamionkowski and K. Griest, *Phys. Rep.* **267**, 195 (1996).
 - [10] V. Bernard, L. Elouadrhiri and U.-G. Meißner, *J. Phys. G* **28**, R1 (2002).
 - [11] C. E. Carlson and J. L. Poor, *Phys. Rev. D* **36**, 2169 (1987).
 - [12] T. S. Park, L. E. Marcucci, R. Schiavilla, M. Viviani, A. Kievsky, S. Rosati, K. Kubodera, D.-P. Min and M. Rho, *Phys. Rev. C* **67**, 055206 (2003).
 - [13] G. Prézeau, A. Kurylov, M. Kamionkowski and P. Vogel, *Phys. Rev. Lett.* **91**, 231301 (2003).
 - [14] E. Epelbaum, H.-W. Hammer and U.-G. Meißner, *Rev. Mod. Phys.* **81**, 1773 (2009).
 - [15] B. Friman and A. Schwenk, in *From Nuclei to Stars*, Festschrift in Honor of Gerald E. Brown, Ed. S. Lee (World Scientific, 2011), arXiv:1101.4858.
 - [16] J. W. Holt, N. Kaiser and W. Weise, *Phys. Rev. C* **79**, 054331 (2009); *ibid.* **81**, 024002 (2010).
 - [17] J. D. Walecka, *Theoretical Nuclear and Subnuclear Physics* (Oxford University Press, 1995), see p. 119.
 - [18] E. Caurier, G. Martínez-Pinedo, F. Nowacki, A. Poves and A. P. Zuker, *Rev. Mod. Phys.* **77**, 427 (2005).
 - [19] P. Toivanen, M. Kortelainen, J. Suhonen and J. Toivanen, *Phys. Rev. C* **79**, 044302 (2009).
 - [20] K. Sieja, G. Martínez-Pinedo, L. Coquard and N. Pietralla, *Phys. Rev. C* **80**, 054311 (2009).
 - [21] M. T. Ressel and D. J. Dean, *Phys. Rev. C* **56**, 535 (1997).
 - [22] A. T. Gallant *et al.*, *Phys. Rev. Lett.* **109**, 032506 (2012) and references therein.

TABLE I. Fits to the structure factors S_{00} , S_{11} and S_{01} for spin-dependent WIMP elastic scattering off ^{129}Xe and ^{131}Xe nuclei, including 1b and 2b currents as in Figs. 2 and 3. For the 1b+2b current results, both the central value of the theoretical error band was used for the fits (first rows) and the limits of the band (second rows). The fitting function of the dimensionless variable $u = p^2 b^2 / 2$ is $S_{ij}(u) = e^{-u} \sum_{n=0}^9 c_{ij,n} u^n$. The rows give the coefficients $c_{ij,n}$ of the u^n terms in the polynomial.

^{129}Xe					
$u = p^2 b^2 / 2, b = 2.2853 \text{ fm}$					
$e^{-u} \times$	S_{00}	$S_{11} \text{ (1b)}$	$S_{11} \text{ (1b+2b)}$	$S_{01} \text{ (1b)}$	$S_{01} \text{ (1b+2b)}$
1	0.054731	0.048192	0.02933	-0.102732	-0.0796645
u	-0.146897	-0.148361	-0.0905396	0.297105	0.231997
u^2	0.182479	0.202347	0.122783	-0.387513	-0.304198
u^3	-0.128112	-0.151853	-0.0912046	0.281816	0.222024
u^4	0.0539978	0.0674284	0.0401076	-0.122388	-0.096693
u^5	-0.0133335	-0.0179342	-0.010598	0.0317668	0.0251835
u^6	0.00190579	0.00286368	0.00168737	-0.00492337	-0.00392356
u^7	-1.48373×10^{-4}	-2.65795×10^{-4}	-1.56768×10^{-4}	4.39836×10^{-4}	3.53343×10^{-4}
u^8	5.11732×10^{-6}	1.29656×10^{-5}	7.69202×10^{-6}	-2.02852×10^{-5}	-1.65058×10^{-5}
u^9	-2.06597×10^{-8}	-2.47418×10^{-7}	-1.48874×10^{-7}	3.46755×10^{-7}	2.88576×10^{-7}
$e^{-u} \times$		$S_{11} \text{ (1b+2b band)}$		$S_{01} \text{ (1b+2b band)}$	
1		0.0360513	0.0226064	-0.0888962	-0.070431
u		-0.110705	-0.0703558	0.257562	0.20644
u^2		0.150026	0.0954932	-0.336681	-0.271749
u^3		-0.111714	-0.0706386	0.245328	0.198772
u^4		0.0493115	0.0308683	-0.106746	-0.0866783
u^5		-0.0130745	-0.00810917	0.0277603	0.0226217
u^6		0.00208705	0.00128522	-0.00431334	-0.00353705
u^7		-1.94174×10^{-4}	-1.19086×10^{-4}	3.86604×10^{-4}	3.20472×10^{-4}
u^8		9.52295×10^{-6}	5.84562×10^{-6}	-1.79013×10^{-5}	-1.51335×10^{-5}
u^9		-1.83523×10^{-7}	-1.13885×10^{-7}	3.06893×10^{-7}	2.70785×10^{-7}
^{131}Xe					
$u = p^2 b^2 / 2, b = 2.2905 \text{ fm}$					
$e^{-u} \times$	S_{00}	$S_{11} \text{ (1b)}$	$S_{11} \text{ (1b+2b)}$	$S_{01} \text{ (1b)}$	$S_{01} \text{ (1b+2b)}$
1	0.0417889	0.0368132	0.022446	-0.0784478	-0.0608808
u	-0.111171	-0.118361	-0.0733931	0.230484	0.181473
u^2	0.171966	0.176773	0.110509	-0.343106	-0.272533
u^3	-0.133219	-0.137987	-0.0868752	0.263525	0.211776
u^4	0.0633805	0.063821	0.0405399	-0.120946	-0.0985956
u^5	-0.0178388	-0.0176743	-0.0113544	0.0331754	0.027438
u^6	0.00282476	0.00287653	0.00187572	-0.00528724	-0.0044424
u^7	-2.31681×10^{-4}	-2.63605×10^{-4}	-1.75285×10^{-4}	4.6475×10^{-4}	3.97619×10^{-4}
u^8	7.78223×10^{-6}	1.23239×10^{-5}	8.40043×10^{-6}	-2.00407×10^{-5}	-1.74758×10^{-5}
u^9	-4.49287×10^{-10}	-2.17839×10^{-7}	-1.53632×10^{-7}	2.90375×10^{-7}	2.55979×10^{-7}
$e^{-u} \times$		$S_{11} \text{ (1b+2b band)}$		$S_{01} \text{ (1b+2b band)}$	
1		0.0275713	0.0173191	-0.067911	-0.0538485
u		-0.0891521	-0.0576174	0.20071	0.162246
u^2		0.134094	0.0868883	-0.301325	-0.24379
u^3		-0.105277	-0.0684403	0.233566	0.190041
u^4		0.0490864	0.0319771	-0.108494	-0.0887141
u^5		-0.0137279	-0.00897632	0.0301064	0.0247694
u^6		0.00226103	0.00148964	-0.00485087	-0.0040324
u^7		-2.10252×10^{-4}	-1.40246×10^{-4}	4.30628×10^{-4}	3.64368×10^{-4}
u^8		1.0004×10^{-5}	6.79325×10^{-6}	-1.86527×10^{-5}	-1.62836×10^{-5}
u^9		-1.80793×10^{-7}	-1.26396×10^{-7}	2.63842×10^{-7}	2.48126×10^{-7}